

Properties of dissipative Floquet Majorana modes using a quantum dot

Nicolò Forcellini,^{1,*} Zhan Cao,¹ and Dong E. Liu^{2,1,3}

¹*Beijing Academy of Quantum Information Sciences, Beijing 100193, China*

²*State Key Laboratory of Low Dimensional Quantum Physics,*

Department of Physics, Tsinghua University, Beijing, 100084, China

³*Frontier Science Center for Quantum Information, Beijing 100084, China*

(Dated: January 23, 2023)

We study the electronic conductance of dissipative Floquet Majorana zero modes (FMZMs) in a periodically driven nanowire coupled to a quantum dot. We use a numerical method which can accurately take into account the dissipation effects from the superconducting bath, which causes the FMZMs to have a finite lifetime. Our results show that, in the weak nanowire-dot coupling regime, the peak conductance at zero temperature of the resonant dot can be well approximated by a universal function of the FMZM lifetime rescaled with the nanowire-dot coupling strength: For a long FMZM's lifetime, the conductance approaches the characteristic quantized value of $G = e^2/2h$, whereas $G \rightarrow e^2/h$ (uncoupled dot) as the FMZMs' lifetime goes to zero. In principle, our method can be used to test the presence and lifetime of FMZMs in such devices, which is key for any practical application of these topological states.

I. INTRODUCTION

Topological superconductors can host zero-energy modes, also called *Majorana zero modes* (MZMs) [1, 2], which, if experimentally engineered, have the potential to make topological quantum computation practical [3, 4] due to their non-Abelian braiding properties [4–7]. MZMs have, so far, proven to be extremely difficult to engineer experimentally. A possible platform is given by semiconductor nanowires with spin-orbit coupling proximitized to an s-wave superconductor (SC) [8–12]. Seeking the realization of Majorana modes in such devices has been the subject of extensive research in the past decade, with recent experimental progresses [13–26].

Topological states of matter and nontrivial band structures can also be accessed through Floquet engineering, i.e., the control of quantum systems through the application of a controlled periodic drive [27–48]. The characteristic “replicated” Floquet band structure in energy space for solid-state systems has been experimentally verified through time and angle-resolved photoemission spectroscopy [49–51]. In particular, Floquet methods can induce a topological phase transition while the static system is topologically trivial, as for the case of Floquet Majorana modes (FMZMs), the periodically-driven equivalent of MZMs [34, 36, 37]. The study of non-equilibrium phases of matter that can exhibit FMZMs has been an active field of research in the past years, as it connects the field of topology in condensed matter to problems in non-equilibrium physics such as prethermalization, thermalization and disorder in open/closed quantum systems, time crystals, etc. [52–59]. Specifically, open quantum systems can show a complicated behaviour in particle

statistics, depending on the details of the bath and the system-bath coupling [60–63]. In addition, recent works about realistic Floquet superconductors [64] and on dissipative FMZMs in nanowires [65] highlight the importance of taking the SC bath-nanowire coupling into account: In the presence of dissipation, while bosonic condensation in the SC survives in the presence of a periodic drive, fermionic quasiparticles, including FMZMs, acquire a finite lifetime, which the standard Floquet theorem cannot correctly capture.

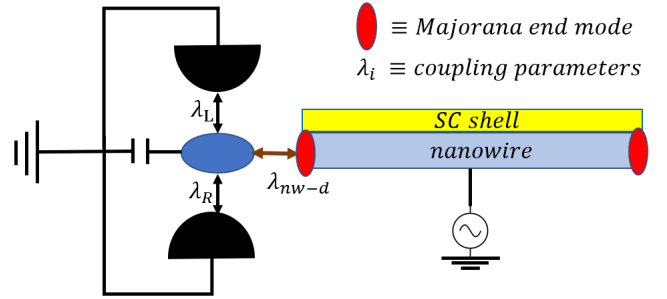


FIG. 1: Setup of the proposed device: the nanowire is periodically driven with frequency Ω , with one of its ends coupled to a quantum dot through an effective coupling λ_{nw-d} . The dot itself is connected to external leads L and R to measure its conductance.

Therefore, in this work we further investigate the lifetime of dissipative Floquet Majorana zero modes (FMZMs) [65]. The effects of dissipation from the superconducting bath are taken into account using the Floquet-Keldysh formalism, which allows to realistically model the SC bath embedding the system [64–66]. We model a setup which would allow to experimentally probe the lifetime of the dissipative FMZMs, see Fig. 1. The setup consists of a quantum dot (QD) resonantly coupled

* nforcellini@baqis.ac.cn

to a FMZM located at the end of a nanowire, which is periodically driven with frequency Ω ; two external leads (L,R) are used to measure the QD electronic conductance. We show that reducing the FMZMs' lifetime by increasing the periodic drive amplitude in the nanowire leads to a transition in the QD single-spin conductance from $G = e^2/2h$ (Majorana mode signature, see e.g. [67]) to $G = e^2/h$ (resonant uncoupled dot).

In the weak nanowire-dot coupling regime, the conductance in the presence of dissipation in the nanowire-SC system can be modeled by using a finite-lifetime Majorana zero mode (MZM) toy model, with the conductance being a universal function of the FMZM lifetime, rescaled with respect to the nanowire-dot coupling strength. However, for a stronger coupling the Floquet structure of the FMZMs' Green's function needs to be taken into account: The functional form of the conductance becomes more complex and deviates from the simpler toy model for short FMZMs' lifetimes, maintaining the same asymptotic behaviour for long lifetimes.

Therefore, we show through our results that the QD conductance can be used as a signature of the presence of dissipative FMZMs in periodically driven topological nanowires, and it can also be used as a measure of FMZMs' lifetime in such devices.

The paper is organized as follows: In section II we introduce the model of the driven-dissipative nanowire coupled to a QD, and derive the expression of the QD Floquet conductance. In section III, we present and discuss our numerical results on the QD spectrum and conductance, as well as introducing a toy model that allows for a good physical understanding of the numerical results. Finally, in section IV, we report our conclusions.

II. MODEL

A. Superconducting nanowire

Consider a one-dimensional (1D) semiconducting nanowire (SM) in proximity of an s-wave superconducting (SC) bath. We introduce a periodic drive in the SM region. The 1D Bogoliubov-de Gennes (BdG) Hamiltonian representing such a system is given by

$$H(t) = H_{nw}(t) + H_{sc} + H_c; \quad (1)$$

the SM Hamiltonian, in real space, is

$$H_{nw}(t) = \int_0^L dx \psi_x^\dagger \left[\left(\frac{p_x^2}{2m} - \mu + 2A \cos(\Omega t) \right) \sigma_0 \tau_z - \alpha p_x \sigma_y \tau_z + V_z \sigma_z \tau_z \right] \psi_x, \quad (2)$$

with spinor representation $\psi_x = (c_{x\uparrow}, c_{x\downarrow}, c_{x\uparrow}^\dagger, c_{x\downarrow}^\dagger)^T$, where $c_{x\uparrow/\downarrow}$ annihilates an up/down-spin electron at location x on the nanowire of length L ; μ is the chemical

potential, A and $\Omega = 2\pi/\tau$ are the amplitude and frequency of the periodic drive, V_z is the Zeeman energy and α is the spin-orbit coupling strength. σ_μ and τ_μ indicate the Pauli matrices in the spin and Nambu spaces, respectively. Note that we assume the nanowire to be uniform, and therefore effects such as the appearance of non-topological edge states such as "quasi-Majorana modes" (QMMs), which can be induced by disorder and other imperfections in the nanowire [68–73], are not considered. The study of QMMs for this setup goes beyond the scope of the present work, and shall be left for a follow-up study. Moreover, we assume that the system is in the nonequilibrium steady-state, meaning that energy transfer/heating influx and outflux between the system and the bath are balanced [28, 29, 65, 66], leading to a Green's function (GF) periodic with the period τ of the drive $Q(t, t') = Q(t + \tau, t' + \tau)$.

The Hamiltonian of the SC bath is, in the mean-field BdG form in momentum space $H_{sc} = \sum_q \phi_q^\dagger (\epsilon_q \tau_z - \Delta \sigma_y \tau_y) \phi_q$, where Δ is the SC gap, and $\phi_q = (a_{q\uparrow}, a_{q\downarrow}, a_{-q\uparrow}^\dagger, a_{-q\downarrow}^\dagger)^T$, where $a_{q\uparrow/\downarrow}$ is the annihilation operator for spin up/down electrons of momentum q in the SC bath. The SC-nanowire coupling H_c is modeled as follows: Firstly, the nanowire Hamiltonian is discretized with lattice spacing a becoming

$$H_{nw}(t) = \frac{1}{2} \sum_i \psi_i^\dagger \{ (2t_h - \mu + 2A \cos \Omega t) \sigma_0 \tau_z + V_z \sigma_z \tau_z \} \psi_i - \left[\psi_{i+a}^\dagger \left(t_h \sigma_0 + \frac{\alpha}{2a} \sigma_y \right) \tau_z \psi_i + H.c. \right] \quad (3)$$

where the hopping constant $t_h \equiv \hbar^2/2ma^2$.

Then, the Markovian approximation [65], through which correlations in the bath are neglected, allows to couple each site of the chain to independent and identical SC baths $H_{sc,i} = \sum_q \phi_{qi}^\dagger (\epsilon_{qi} \tau_z - \Delta \sigma_y \tau_y) \phi_{qi}$. Hence, the coupling Hamiltonian can be expressed as

$$H_c = \sum_{i,q,\sigma} V \left(c_{i,\sigma}^\dagger a_{q,\sigma} + a_{q,\sigma}^\dagger c_{i,\sigma} \right). \quad (4)$$

The SC gap Δ and the nanowire-SC coupling V are taken to be real, positive numbers without loss of generality. The external degrees of freedom can then be integrated out as shown in [65] using the Floquet theorem, and the resulting effective Floquet Hamiltonian and on-site Green's function are reported in the Appendix. The main point is that a finite SC gap Δ broadens the quasiparticle spectrum, representing dissipation caused by the SC bath. On the other hand, the non-dissipative limit $\Delta \rightarrow \infty$ is equivalent to the introduction of a simple induced gap term $\Delta_{ind} \sigma_y \tau_y$ in the nanowire, with induced order parameter $\Delta_{ind} = \pi \rho_F V^2$, where we set $\pi \rho_F = 1$ as the density of states (DOS) of the SC bath. See the Appendix and [65] for more details on the dissipation model and the large- Δ non-dissipative limit.

B. Coupling the dot

Consider the undriven QD coupled to one of the ends of the nanowire through some effective hopping λ_{nw-d} [67]

$$H_d = \sum_{\sigma} \epsilon_d d_{\sigma}^{\dagger} d_{\sigma} + \lambda_{nw-d} \sum_{\sigma} (d_{\sigma}^{\dagger} c_{L,\sigma} + h.c.) + \sum_{k,\alpha=L,R,\sigma} \lambda_{\alpha\sigma} (c_{k\alpha\sigma}^{\dagger} d_{\sigma} + h.c.) + V_z^d (d_{\uparrow}^{\dagger} d_{\uparrow} - d_{\downarrow}^{\dagger} d_{\downarrow}). \quad (5)$$

In the above, ϵ_d is the dot level, and c_L is the annihilation operator for the last site of the nanowire. The two leads labeled as left (L) and right (R) have Hamiltonian $H_{leads} = \sum_{k,\alpha=L,R} c_{k\alpha\sigma}^{\dagger} c_{k\alpha\sigma}$ and couple to the dot with a width $\Gamma_{\alpha\sigma} \equiv 2\pi |\lambda_{\alpha\sigma}|^2 \rho_{Fl}$, where the lead DOS $2\pi \rho_{Fl} = 1$ is assumed to be constant. $c_{k\alpha\sigma} (d_{\sigma})$ denotes the electron annihilation operator for the leads (QD). V_z^d is the Zeeman splitting for the dot, which might be different from V_z of the nanowire, or, when assuming that the QD and nanowire materials are the same, can be set to have the same value. In any case, we assume that the Zeeman energy is the largest scale in the QD, and therefore we can consider only one spin channel, ignoring any electron-electron interaction in the above Hamiltonian. Moreover, we tune the QD such that the energy of the spin- \downarrow electron $\epsilon_d - V_z^d = 0$, allowing this state to be resonant with the FMZM.

From this model, and following the method described in [65], we use the recursive Floquet-Green's function technique to obtain the relevant components of the dot Green's function used for our calculations –see the Appendix for more details.

In this work we investigate the QD conductance due to its coupling to dissipative FMZMs of finite lifetime τ_{FM} : As mentioned in the previous section, a finite SC gap Δ induces dissipation, i.e., a broadening of the quasiparticle spectrum. Our operational definition of the FMZM lifetime is the inverse of the width $\Gamma_{FM} = \tau_{FM}^{-1}$ obtained by fitting the FMZM peak of the spectrum at the end of the nanowire: With the (time-averaged) DOS of a FMZM at the end of the nanowire

$$\nu_{FM}(\omega) = -\frac{1}{\pi} \text{ImTr} \{Q_{FM}^R(0, \omega)\}, \quad (6)$$

and the FMZM Floquet Green's function having the form $Q_{FM}^R(0, \omega) = [\omega - \Sigma_{FM}(\omega)]^{-1}$, then one has, in the zero-frequency approximation,

$$\nu_{FM}(\omega) \propto \frac{\Gamma_{FM}}{\omega^2 + \Gamma_{FM}^2}. \quad (7)$$

Hence, we identify the self-energy $\Sigma_{FM}(\omega = 0) = -i\Im[\Sigma_{FM}(\omega = 0)] = i\Gamma_{FM}$ in the FMZM Green's function as purely imaginary, since the peak of $\nu_{FM}(\omega)$ is

always at $\omega = 0$ for a FMZM. In addition, increasing the driving amplitude A also leads to an increase in dissipation and a decay in quasiparticle lifetime in the nanowire [65]. Hence, we use A as the tuning parameter for FMZMs' lifetime control. For a more detailed discussion on the definition of Floquet Majoranas' lifetime, we refer to [65]. For this work, the above definition suffices.

C. Quantum dot conductance for a Floquet system

The time-dependent current in the left lead is given by

$$I_L(t) = \frac{ie}{\hbar} \sum_{k\sigma} (\lambda_{kL\sigma} c_{kL\sigma}^{\dagger} d_{\sigma} - \lambda_{kL\sigma}^* d_{\sigma}^{\dagger} c_{kL\sigma}), \quad (8)$$

with the equivalent definition for the current through R. Details of the derivation of the expression for the current $I(t) = I_L(t) + I_R(t)$ through the QD using Floquet-Keldysh field theory are left to the Appendix. Here, we report the final expression for the zero-bias time-averaged conductance ($G = d\langle I \rangle / dV|_{V \rightarrow 0}$)

$$G = -\frac{2e^2}{\hbar} \int \frac{d\omega}{2\pi} \frac{\Gamma_L \Gamma_R}{\Gamma_L + \Gamma_R} \text{ImTr} \{Q_{dd}^R(0, \omega)\} \left(-\frac{\partial n_F}{\partial \omega} \right). \quad (9)$$

In the above, $n_F(\omega)$ is the Fermi-Dirac distribution, and $Q_{dd}^R(0, \omega)$ is the 0th Fourier component (time average) of the retarded component of the QD GF defined as –with $t_{rel} = t - t'$ –

$$Q(n, \omega) = \frac{1}{\tau} \int^{\tau} dt \int dt_{rel} e^{-in\Omega t} e^{-i\omega t_{rel}} Q(t, t') \quad (10)$$

for $n = 0$, where we made use of the periodicity of the GF [66]. Since in our system we assume that the driving frequency Ω is very high compared to the other energy scales, it is sufficient to compute the time-averaged conductance. Eq. 9 can be seen as the Floquet generalization of the static QD conductance [67].

As a special case, consider symmetric coupling to the leads $\Gamma_L = \Gamma_R = \Gamma$ leading to the peak conductance (as the temperature $T \rightarrow 0$)

$$G_{peak} = -\frac{e^2}{\hbar} \Gamma \text{ImTr} \{Q_{dd}^R(0, \omega \rightarrow 0)\}. \quad (11)$$

For our numerical calculations of the conductance, we only select the spin \downarrow -electron. From now on, G_{peak} will be referred to as G , and Eq. 11 will be used to produce our numerical results for the time-averaged QD conductance.

III. RESULTS AND DISCUSSION

A. Quantum dot spectral function

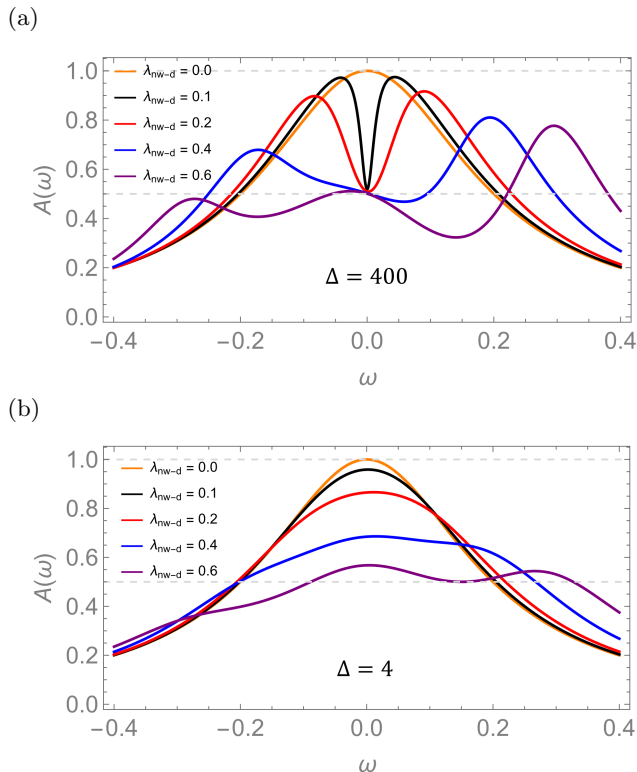


FIG. 2: Quantum dot spectrum when coupled to (a) a non-dissipative FMZM, note the value $A(0) = 1/2$, expected from Majorana modes for any $\lambda_{nw-d} \neq 0$, and (b) a dissipative FMZM, with the same parameters as in (a) except for the SC Gap Δ . Note how the $1/2$ -value at $\omega = 0$ is lost, with $A(0) \rightarrow 1$ for small λ_{nw-d} . For the calculations, $\epsilon_d = V_z^d$, placing the \downarrow -electron at zero energy. $\Gamma_L = \Gamma_R = \Gamma = 0.1$, $t_h = 2.0$ (bandwidth $D = 4t_h = 8.0$), $\mu = -2.0$, $\alpha = 3.0$, $V_z = V_z^d = 4.0$, $V = 1.2$, $A = 3.0$ and $\Omega = 12.0$.

As a first step, in Fig. 2 we investigate the single-spin spectral function of the dot $A_\downarrow(\omega) \equiv -\Gamma \Im \left\{ Q_{dd,\downarrow}^R(0, \omega) \right\}$ –for simplicity we will drop the \downarrow -label. In Fig. 2a, in the non-dissipative limit, the dot spectrum has the same characteristics of a quantum dot coupled to a (non-Floquet, static) Majorana zero mode (MZM) with the same setup [67]: The dot spectral function $A(0) = 1/2$ whenever the MZM is coupled to the dot, independently of the coupling strength, and $A(0) = 1$ with $\lambda_{nw-d} = 0$ (resonant isolated dot). This translates in a peak conductance with a value $G = e^2/2h$, which is a signature of MZMs [67]. This is in fact not surprising: Expressing

a FMZMs as a Bogoliubov quasiparticle operator

$$\eta^\dagger(x, t) = \int dx \left[u(x, t) \hat{\psi}_x^\dagger + v(x, t) \psi_x \right], \quad (12)$$

it has been proved, both numerically and using theoretical arguments, that FMZMs are MZMs at all times [36, 37, 74]. In the above expression the functions $u(x, t)$ and $v(x, t)$ represent the spatial and temporal modulation of the zero modes, which, albeit time-dependent, are localised at the end of the nanowire at all times.

On the other hand, Fig. 2b shows the spectrum in the presence of a dissipative FMZM: In this case, the $A(0) = 1/2$ -signature is generally lost, with a decreasing λ_{nw-d} leading to $A(0) \rightarrow 1$. Intuitively, this is due to the FMZM having acquired a finite lifetime due to dissipation, which approaches the uncoupled limit $A(0) \rightarrow 1$ as the lifetime gets shorter and/or the coupling λ_{nw-d} gets weaker. λ_{nw-d} should be kept small enough: with the current parameters –see caption of Fig. 2– the induced gap parameter is $\Delta_{ind} = 1.44$, and therefore we must have $\lambda_{nw-d} < \Delta_{ind}$ to limit the undesired influence of modes above the gap. In our calculations, the nanowire has a length $L = 200$ sites, and we set the Floquet cutoff $N_F = 10$ to ensure convergence of the numerics [65]. The parameters used in this work and reported in Fig. 2 and 5 agree with previous works on dissipative and non-dissipative FMZMs [37, 65], and are consistent with proposals of FMZM realization in cold-atom systems [34].

B. Conductance and FMZMs' lifetime

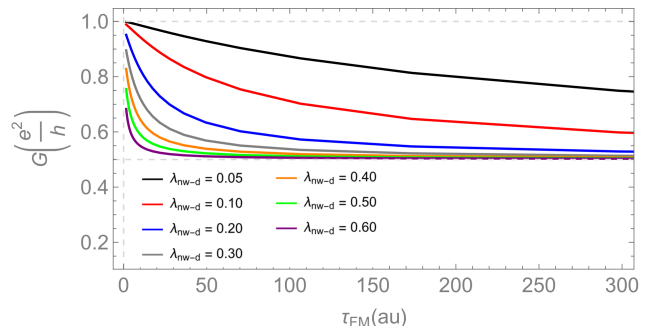


FIG. 3: Conductance G from Eq. 11 as a function of the FMZM lifetime τ_{FM} (arbitrary units), as the nanowire-dot coupling λ_{nw-d} is changed. With a sufficiently long lifetime, the conductance G is stabilized around the topological signature $G = e^2/2h$. A larger value for λ_{nw-d} , meaning a stronger coupling to the finite-lifetime FMZM, leads to a more stable signal around $G = e^2/2h$. Parameters as in Fig. 2 ($\Omega = 12.0$, etc.), with amplitudes $0 \leq A \leq 5.2$, which allows to tune the lifetime τ_{FM} in the x-axis, and $N_F = 10$ Floquet matrix cutoff.

In order to better understand the conductance signal of the dissipative FMZMs, we show in Fig. 3 the val-

ues of G as a function of FMZM lifetime τ_{FM} for different λ_{nw-d} . By increasing the strength A of the Floquet drive (and shortening the FMZM lifetime τ_{FM}) we find a transition between $G = e^2/2h$, indicating the presence of a Floquet Majorana mode, to $G = e^2/h$, which is the conductance of an uncoupled dot resonant at zero energy. A stronger coupling stabilizes the conductance signal around the Majorana signature $G = e^2/2h$. In the following, we start from the simplest toy model for dissipative Majorana modes in order to better analyze the numerical results.

1. Toy model of a dissipative Majorana mode

Consider the following toy model for a normal MZM coupled to the dot. The effective Hamiltonian for the single-spin dot-MZM system is

$$H = H_{leads} + H_T + H_{QD-MZM}, \quad (13)$$

where

$$H_{QD-MZM} = \epsilon_d d^\dagger d + \lambda_{nw-d} (d - d^\dagger) \eta_1 + i\delta \eta_1 \eta_2, \quad (14)$$

with δ being the exponentially small coupling $\delta \sim e^{-L/\xi}$ with coherence length $\xi = v_F/\Delta_{ind}$. Here, we set $\delta = 0$ to isolate one of the Majoranas. H_{leads} and H_T are the single-spin versions of the lead and lead-dot coupling Hamiltonians previously defined after Eq. 5. In order to impose a finite lifetime for η_1 , we assign it a width $\Gamma_M(\omega)$ in its GF $Q_\eta^R(\omega) = C_0/[\omega + i\Gamma_M(\omega)]$, where C_0 is a normalization constant.

Assuming symmetric coupling to the leads $\Gamma_L = \Gamma_R = \Gamma$ and $\epsilon_d = 0$, the retarded component $Q_{dd}^R(\omega)$ for this toy model is given by

$$Q_{dd}^R(\omega) = \frac{\left[1 - \frac{C_0 |\lambda_{nw-d}|^2}{(\omega + i\Gamma_M(\omega))(\omega + 2i\Gamma)}\right]}{(\omega + 2i\Gamma) \left[1 - \frac{2C_0 |\lambda_{nw-d}|^2}{(\omega + i\Gamma_M(\omega))(\omega + 2i\Gamma)}\right]}. \quad (15)$$

This leads to G with the following simple form

$$G(\tilde{\lambda}) = \frac{e^2}{h} \frac{1 + C_0 |\tilde{\lambda}|^2 / 2\Gamma}{1 + C_0 |\tilde{\lambda}|^2 / \Gamma}, \quad (16)$$

where $|\tilde{\lambda}|^2 = |\lambda_{nw-d}|^2 / \Gamma_M(\omega \rightarrow 0) \sim |\lambda_{nw-d}|^2 \tau_{FM}$. Hence, we found that, given a certain Γ coupling strength with the leads, G is a universal function of the rescaled coupling $\tilde{\lambda}$. This coupling represents the two competing energy/timescales of the nanowire-QD system: MZM lifetime τ_M and the inverse of the nanowire-QD coupling strength $\sim |\lambda_{nw-d}|^2$.

We can easily check that the function has the expected behaviour, with the main features of the conductance curves that can be seen by inspection of Eq. 16: For a perfect MZM with $\tau_M \rightarrow \infty$, $G_{peak} = e^2/h$ if the QD is

decoupled from the MZM, while $G_{peak} = e^2/2h$ for any finite λ_{nw-d} . For a finite τ_M , $G_{peak} > e^2/2h$. Specifically, reducing τ_M would smoothly increase the peak conductance to e^2/h . Moreover, a larger λ_{nw-d} brings G_{peak} closer to the quantized value $e^2/2h$, just as observed in Fig. 3. However, since Eq. 16 can only model MZMs, in the next section we modify the toy model to include the Floquet structure.

2. Floquet Green's function correction

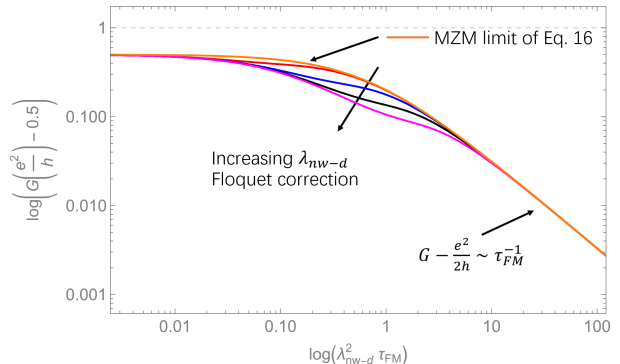


FIG. 4: Log-Log plot of the conductance $G - e^2/2h$ from Eq. 20 using our toy model corrected for the Floquet structure of the FMZM Green's function, Eq. 17. In this plot, $C_k \sim k^{-\alpha}$, $\alpha = 2$. The figure shows that, with increasing λ_{nw-d} , the curve deviates from the low- λ_{nw-d} limit of Eq. 16, which is shown in orange, only for small enough lifetimes. The values set for λ_{nw-d} are 1.0 (red line, almost overlapping with the orange line), 2.0 (blue) and 3.0 (black) and 4.0 (magenta). The values are chosen arbitrarily in order to show the qualitative behavior due to the Floquet structure, with $\Omega = 12.0$.

Due to their time-periodicity, the FMZMs of Eq. 12 can be expanded as $\eta(t) = \sum_n e^{-in\Omega t} \eta_n$, and since their quasienergy $\epsilon_\alpha = 0$, the Green's function is given by

$$Q_\eta^R(n, \omega) = \sum_{k=-\infty}^{\infty} \frac{\eta_{k+n}(\eta_k)^*}{\omega - k\Omega + i\Gamma_M(\omega)}, \quad (17)$$

where the $\Gamma_M(\omega)$ must be the same for each k due to the Floquet theorem, as shown in [65]. By definition, we have $\eta^\dagger(t) = \eta(t)$, and therefore $(\eta_n)^* = \eta_{-n}$. Hence, for $n = 0$ the Green's function can be written as

$$Q_\eta^R(0, \omega) = \frac{C_0}{\omega + i\Gamma_M(\omega)} + \sum_{k=1}^{\infty} \frac{2C_k(\omega + i\Gamma_M(\omega))}{(\omega + i\Gamma_M(\omega))^2 - (k\Omega)^2}, \quad (18)$$

where $C_k \equiv \eta_k(\eta_k)^*$, so that $C_k \geq 0$. These k -dependent factors can be considered as decaying as a function of k , due to the properties of the Fourier series. For our numerical calculations, we set $C_k \sim k^{-\alpha}$, $\alpha = 2$. Different choices for the form of the decaying C_k lead to qualitatively similar results.

The dot Green's function becomes

$$Q_{dd}^R(\omega) = \frac{\left[1 - \frac{|\lambda_{nw-d}|^2}{(\omega+2i\Gamma)} Q_\eta^R(0, \omega)\right]}{(\omega+2i\Gamma) \left[1 - \frac{2|\lambda_{nw-d}|^2}{(\omega+2i\Gamma)} Q_\eta^R(0, \omega)\right]}. \quad (19)$$

From this expression, the generalization of Eq. 16 is easily obtained as

$$G(\tilde{\lambda}) = \frac{e^2}{h} \frac{1 + |\tilde{\lambda}|^2/2\Gamma \left(A^0 + \sum_{k=1}^{\infty} \frac{2A^k \Gamma_M^2}{\Gamma_M^2 + (k\Omega)^2}\right)}{1 + |\tilde{\lambda}|^2/\Gamma \left(A^0 + \sum_{k=1}^{\infty} \frac{2A^k \Gamma_M^2}{\Gamma_M^2 + (k\Omega)^2}\right)}, \quad (20)$$

where $\Gamma_M \equiv \Gamma_M(\omega \rightarrow 0)$. Note that the introduction of the energy scale defined by $\hbar\Omega$ does not allow G to be a universal function of the dimensionless parameter $\tilde{\lambda}$, since the expression in brackets has a dependence on the FMZM width Γ_M . In the $\Omega \rightarrow \infty$ -limit, the expression reduces to the previous model. We can also check the relevant limits of Eq. 20 in the same way that we did for Eq. 16: For the uncoupled dot, $G = e^2/h$, and the large- τ_{FM} limit ($\Gamma_M \rightarrow 0$) leads to $G = e^2/2h$, with the Floquet contribution (second term in the bracket) vanishing. This leads to a $G(\tilde{\lambda})$ as reported in Fig. 4. The results show a deviation from the form of Eq. 16 for shorter lifetimes, while maintaining the same $G - 1/2 \sim \tau_{FM}^{-1}$ behavior for long lifetimes, in agreement with our numerical results.

To summarize, in this section we showed that the conductance through a resonant quantum dot as a function of the rescaled coupling/lifetime $|\lambda_{nw-d}|^2 \tau_{FM}$ has a characteristic functional form, which is almost identical when the dot is coupled to either dissipative MZMs or FMZMs, with the conductance curves differing only for short lifetimes and strong enough nanowire-dot coupling. In particular, given the possibility of tuning of the FMZMs' lifetime and the nanowire-dot coupling strength, our results provide a signature for the presence and stability—in terms of their lifetimes—of FMZMs in topological nanowires: The QD conductance should behave as shown in Figs 3 and 4 and as described by Eq.s 16 and 21. An assumption that we make in the model is the one of a resonant dot: If the QD energy level $\epsilon_d \neq 0$, then the $G(\tau_{FM} \rightarrow 0) < e^2/h$. It is in principle always possible to tune the QD in such a way by measuring its conductance when uncoupled from the nanowire.

In the next and final section, we briefly explore how the QD conductance is modified if other modes in the nanowire also couple to the QD; this can happen in non-ideal experimental conditions.

C. Soft SC gap: normal fermion coupling

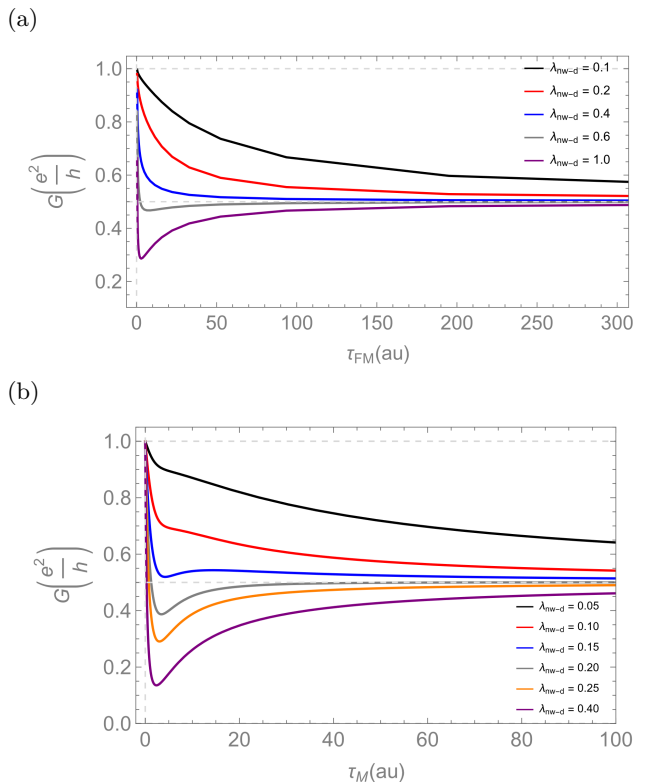


FIG. 5: (a) Same plot as Fig. 3 showing $G < e^2/2h$ for short- τ_{FM} and large λ_{nw-d} , where the model parameters have been modified to get FMZMs with smaller $\Delta_{ind} = 0.64$. Specifically, $t_h = 1.0$ ($D = 4.0$), $\alpha = 1.5$, $V_z = V_z^d = 1.2$, $V = 0.8$, $\Omega = 6.0$, and $0 \leq A \leq 5.2$ as in Fig. 3, with a Floquet matrix cutoff $N_F = 20$. (b) $G(\tau_M)$ from Eq. 22 for the toy model with an additional off-resonant fermion: we can see that the model can qualitatively reproduce the large- λ short-lifetime behavior shown in (a). Eq. 22 is computed with $\Gamma = 0.1$, $\delta = 0.3$.

A setting in which the undesired coupling could happen is the case in which the nanowire-dot coupling gets too large, the coupling of states above the induced gap can affect the value of the conductance. For instance, this effect can manifest itself when engineering very short FMZMs' lifetimes, corresponding to larger amplitudes in the drive, as explained in section II.B and as established in [65]: in such a case, the spectrum in the nanowire is broadened and the SC gap derived from the Floquet GF becomes soft [64]. The effect on the conductance is shown in Fig. 5a, where we modify our model parameters and we set some $\lambda_{nw-d} \gtrsim \Delta_{ind}$: the numerical results show values $G < e^2/2h$ when approaching shorter FMZM lifetimes. However, these conductance curves show a minimum for small τ_{FM} , reverting to $G \rightarrow e^2/h$ for $\tau_{FM} \rightarrow 0$. A value of $G = 0$ is a signature of a dot coupled to a normal

fermion: Hence, the features seen in the figure are probably due to the contribution of states above the induced gap, detected via the strong coupling. However, since such quasiparticles also acquire a finite lifetime due to the drive and dissipation, the limit $G(\tau \rightarrow 0) = e^2/h$ should be maintained.

To analyze this behavior, we add to the MZM a normal fermion with finite width $\Gamma_f(\omega)$ and with finite energy δ –slightly off-resonant with the QD– to the MZM toy model. Hence, the GF becomes –in particle-hole space–

$$Q_{nw}^R(\omega) \approx \begin{pmatrix} \frac{1}{\omega+i\Gamma_M} + \frac{1}{\omega-\delta+i\Gamma_f} & 0 \\ 0 & \frac{1}{\omega+i\Gamma_M} + \frac{1}{\omega+\delta+i\Gamma_f} \end{pmatrix}. \quad (21)$$

In order to derive the simplest possible expression for G capturing the numerics, we make the following assumptions: The lifetimes of both the MZM and the off-resonant fermion are set to be the same $\Gamma_f = \Gamma_M \sim 1/\tau_M$, as well as the nanowire-QD coupling λ_{nw-d} . This leads to the following expression for the conductance (always with $\epsilon_d = 0$):

$$G(\tau_M) = \frac{e^2}{h} \frac{1 + \delta^2 |\lambda_{nw-d}|^2 \tau_M / [2\Gamma(\delta^2 + 1/\tau_M^2)]}{1 + |\lambda_{nw-d}|^2 \left[\frac{\tau_M}{\Gamma} + \frac{1}{(\delta^2 + 1/\tau_M^2)} \left(\frac{1}{\Gamma\tau_M} + \frac{|\lambda_{nw-d}|^2}{2\Gamma^2} \right) \right]}. \quad (22)$$

A plot of the above function is shown in Fig. 5b: The model is able to replicate the small- τ_M /large- λ features of the numerical simulation of 5a, which we can now explain as follows: On the one hand, the FMZM’s lifetime is reduced by dissipation, leading to a reduced “effective coupling” $\tilde{\lambda}$ to the dot. On the other hand, the effect of SC gap softening in the nanowire as the amplitude of the periodic drive is increased can lead to a signal $G \rightarrow 0$ as the dot starts coupling to a normal fermion above the gap. This effect only becomes important as the nanowire-QD coupling $\lambda_{nw-dot} \gtrsim \Delta_{ind}$.

IV. CONCLUSIONS

In this work, we studied for the first time the transport signatures of dissipative FMZMs coupled to a resonant quantum dot. We derived an expression for the conductance from first principles via the Floquet-Keldysh formalism, allowing for a nonperturbative treatment. We showed that the conductance of a dot coupled to a FMZM

shows a characteristic transition from the Majorana signature $G = e^2/2h$ to the uncoupled value $G = e^2/h$ as the FMZM lifetime decays. We showed that the conductance can be well approximated by a universal function of the FMZM lifetime, rescaled with respect to the nanowire-dot coupling strength, despite the fact that the true functional form of the conductance is in fact more complex due to the Floquet structure of the FMZMs’ GF.

Indeed, we showed that the Floquet correction only becomes important at short lifetimes and strong nanowire-dot coupling.

Periodically driven nanowires seem to be a convenient platform for the study of the lifetime and stability of FMZMs, given the simple nanowire-QD coupling setup and tunability of the periodic drive. However, the setup requires a good degree of control and fine-tuning of the coupling strength with the QD, as well as making sure that the induced superconducting gap stays large enough under a strong periodic drive, which might represent obstacles for an experimental realization. Nonetheless, with the above premises, our work illustrates a clear signature for the presence of FMZMs in topological nanowires, even when taking into account the effects of dissipation from the SC bath. In future work, it would be interesting to include more realistic effects in the setup, such as disorder and imperfections in the periodically driven dissipative nanowire to study their effects on electronic transport.

V. ACKNOWLEDGMENTS

We thank Gu Zhang, Zhesen Yang and Qinghong Yang for helpful discussions. The work has been supported by the National Natural Science Foundation of China (Grants No. 11974198 and No. 12004040), Beijing Academy of Quantum Information Sciences, Beijing 100193, China.

Appendix A

1. Nanowire model and recursion method

After integrating out the bath degrees of freedom, the on-site retarded component of the nanowire Floquet Green’s function (GF) takes the form

$$\underline{g}_i(\omega) = \left[\omega - \underline{H}_{eff,i}(\omega) \right]^{-1}. \quad (A1)$$

where the on-site effective Floquet Hamiltonian is

$$\underline{H}_{eff,i}(\omega) = \begin{pmatrix} \dots & & & & & & & & \\ & H_{nw,i} - \Omega + \Sigma_{sc}(\omega + \Omega) & & A\sigma_0\tau_z & & & & & & & \\ & A\sigma_0\tau_z & & & & & & & & & \\ & 0 & & & & & & & & & \\ & & H_{nw,i} + \Sigma_{sc}(\omega) & & & & 0 & & & & \\ & & A\sigma_0\tau_z & & & & A\sigma_0\tau_z & & & & \\ & & 0 & & & & & H_{nw,i} + \Omega + \Sigma_{sc}(\omega - \Omega) & & & \\ & & & & & & & & & & \dots \end{pmatrix}, \quad (\text{A2})$$

where $H_{nw,i} = (2t_h - \mu)\sigma_0\tau_z + V_z\sigma_z\tau_z$ and the bath self-energy term is [65]

$$\Sigma_{sc}(\omega) = V^2 \frac{1}{\sqrt{-(\omega + i\eta)^2 + \Delta^2}} [-(\omega + i\eta) - \Delta\sigma_y\tau_y], \quad (\text{A3})$$

where $\eta = 0^+$ and the bath DoS is assumed to be uniform. For the numerical calculations η is set to a finite positive value, much smaller than any other energy scale in the system. The notation \underline{M} indicates a matrix in Floquet space, which is in principle infinite-dimensional due to the Fourier expansion, and we denote by $[\underline{M}]_{mn}$.

For instance, in Eq. A2 $[\underline{H}_{eff,i}(\omega)]_{nn} = H_{nw,i} + \Sigma_{sc}(\omega - n\Omega) + n\Omega$. In $\underline{H}_{eff,i}(\omega)$ the off-diagonal elements represent the harmonic drive. A value of $\kappa \equiv A/\Omega < 1$ ensures convergence and allows for the truncation of the matrices in the Floquet Hilbert space for any value of Ω , and the matrix dimensions can be kept conveniently small without any appreciable loss of accuracy [65, 66]. Moreover, the $Q(0,\omega)$ -elements of the Floquet GF used in the main text to compute time-averages of observables are extracted from the $[Q_{dd}(\omega)]_{00}$ -component of the Floquet GF matrix. The meaning of the self-energy of Eq. A3 is that it represents dissipation through its ω -dependence, i.e., a broadening of the quasiparticle spectrum via its imaginary part; when $\Delta < \Omega$, the self-energy of $[\underline{H}_{eff,i}(\omega)]_{11/-1-1}$ becomes purely imaginary, which means that ‘‘single-photon’’ Floquet transitions lead to energy-particle exchange directly above the SC bath; when $\Delta > \Omega$, higher-order transitions are necessary and therefore the FMZM lifetime is longer. The non-dissipative limit is found by letting $\Delta \rightarrow \infty$, whence $\Sigma_{sc} = \Delta_{ind}\sigma_y\tau_y$, with the self-energy simply becoming a real-valued induced gap parameter in the nanowire, with $\Delta_{ind} \equiv \rho_F V^2$.

The spectrum and LDoS of the FMZMs at the end of the nanowire can be calculated from the retarded part of the local GF, which is found by using the following recursive matrix equation in the Floquet-Keldysh-BdG space [65]

$$Q_{i+1,i+1}(\omega) = [g_i^{-1}(\omega) - T_{i+1,i} \cdot Q_{i,i}(\omega) \cdot T_{i,i+1}]^{-1}, \quad (\text{A4})$$

where $g_i(\omega)$ is the on-site ‘‘bare’’ GF defined in Eq. A1. The above equation is iterated for $N = 200$ sites in our calculations, with an appropriate N_F Floquet matrix cutoff to ensure convergence. The hopping matrix in the

nanowire is

$$T_{i,i+1} = T_{i+1,i}^T = \begin{pmatrix} -t_h & 0 & -\alpha/2a & 0 \\ 0 & t_h & 0 & \alpha/2a \\ \alpha/2a & 0 & -t_h & 0 \\ 0 & -\alpha/2a & 0 & t_h \end{pmatrix} \quad (\text{A5})$$

which, extended in F-K-BdG space, is simply $T_{i,i+1} = I_{2N_F+1} \otimes I_2 \otimes T_{i,i+1}$.

The quantum dot coupled to the leads of Eq. 5 can be included as an additional site of the recursive chain, which means that we need to perform an additional iteration of Eq. A4 with $g^{-1}(\omega) = \text{diag}[\omega - \epsilon_d - V_z^d + i(\Gamma_L + \Gamma_R), \omega - \epsilon_d + V_z^d + i(\Gamma_L + \Gamma_R), \omega + \epsilon_d + V_z^d + i(\Gamma_L + \Gamma_R), \omega + \epsilon_d - V_z^d + i(\Gamma_L + \Gamma_R)]$ and $T_{i,i+1} = \text{diag}[-\lambda_{nw-d}, \lambda_{nw-d}, -\lambda_{nw-d}, \lambda_{nw-d}]$.

2. Derivation of the current and conductance using Floquet-Keldysh field theory

In order to derive the expression of conductance of Eq. 9 in the main text, one can start from the effective action with current source term [75]

$$S = S_0 + S_{L-D} + S_{source}, \quad (\text{A6})$$

where

$$S_0 = \sum_{kk', \alpha=L,R} \int_C \int_C dt dt' \Psi_{k,\alpha}^\dagger(t) Q_{0,kk'\alpha}^{-1}(t,t') \Psi_{k',\alpha}(t') + \int_C \int_C dt dt' \Psi_d^\dagger(t) Q_{0,dd}^{-1}(t,t') \Psi_d(t'), \quad (\text{A7})$$

and the coupling part of the action is given by

$$S_{L-D} = \sum_{k\alpha} \int_C dt (\lambda_{k\alpha} c_{k\alpha}^\dagger d + h.c.) = \sum_{k\alpha} \int_C dt (\Psi_{k,\alpha}^\dagger(t) \hat{M}_{T,k\alpha} \Psi_d(t) + h.c.), \quad (\text{A8})$$

where we choose to work in the Nambu basis $\Psi_{k,\alpha}^\dagger = (c_{k,\alpha}^\dagger, c_{k,\alpha})/\sqrt{2}$ and $\Psi_d^\dagger = (d^\dagger, d)/\sqrt{2}$; the tunnelling matrix element is $M_{T,k\alpha} = \begin{pmatrix} \lambda_{\alpha k} & 0 \\ 0 & -\lambda_{\alpha k}^* \end{pmatrix}$; $Q_{0,dd}(t,t')$ is the Green's operator for the dot, and $Q_{0,kk'\alpha}(t,t')$ is the Green's function of the lead.

By defining a spinor for the whole space $\Psi^\dagger = (l_{kL}^\dagger, l_{kL}, d^\dagger, d, l_{kR}^\dagger, l_{kR})/\sqrt{2}$, the above action terms can be expressed as

$$S_0 + S_{L-D} = \int_C \int_C dt dt' \Psi^\dagger(t) Q^{-1}(t, t') \Psi(t'), \quad (\text{A9})$$

where the Green's function is

$$Q_{kk'} = \begin{pmatrix} Q_{Lk, Lk'} & Q_{Lk, d} & Q_{Lk, Rk'} \\ Q_{d, Lk'} & Q_{d, d} & Q_{d, Rk'} \\ Q_{Rk, Lk'} & Q_{Rk, d} & Q_{Rk, Rk'} \end{pmatrix}. \quad (\text{A10})$$

Out of these components, for the transport calculations, we only need the Q_{dd} from the dot, as we will show in the following derivation.

Finally, the source term is defined as

$$S_{source} = - \int dt A(t) I_L(t) = - \sum_{a,b=1}^2 \int_{-\infty}^{\infty} dt \bar{\Psi}_a \hat{A}_{ab} \hat{M}_L \Psi_b, \quad (\text{A11})$$

where the spinors and matrices are now in Keldysh space after performing a Larkin-Ovchinnikov rotation, where $\hat{A} = A^q \gamma^q$, $\gamma^q = \sigma_1$, and the Keldysh spinors $\Psi_{1,2}, \bar{\Psi}_{1,2}$ are defined as $\Psi_{1/2} = (\Psi^+ \pm \Psi^-)/\sqrt{2}$ and $\bar{\Psi}_{1/2} = (\bar{\Psi}^+ \mp \bar{\Psi}^-)/\sqrt{2}$ [76, 77]. This source term generates the current through the left lead

$$I_L(t) = \frac{ie}{\hbar} \sum_{k\sigma} (\lambda_{Lk} l_{Lk\sigma}^\dagger d_\sigma - \lambda_{Lk\sigma}^* d_\sigma^\dagger l_{Lk\sigma}) = \bar{\Psi}^\dagger(t) \hat{M}_L \bar{\Psi}(t), \quad (\text{A12})$$

The transport matrix \hat{M}_L is defined as

$$\hat{M}_L = \frac{ie}{\hbar} \begin{pmatrix} 0 & M_L^{12} & 0 \\ M_L^{21} & 0 & 0 \\ 0 & 0 & 0 \end{pmatrix}, \quad (\text{A13})$$

with $M_L^{12} = \begin{pmatrix} \lambda_{Lk} & 0 \\ 0 & \lambda_{Lk}^* \end{pmatrix}$ and $M_L^{21} = \begin{pmatrix} -\lambda_{Lk}^* & 0 \\ 0 & -\lambda_{Lk} \end{pmatrix}$. The generating function is $Z[A] = \int D[\bar{\Psi}\Psi] e^{iS}$, and upon Gaussian integration to linear order in A^q , $\ln Z[A] = \text{Tr} \ln [\hat{1} - QAM] \approx -\text{Tr}[QA^q \gamma^q M_L]$. The current can be expressed as

$$I_L(t) = \frac{i}{2} \frac{\delta \ln Z[A]}{\delta A^q} \Big|_{A^q=0} \approx -\frac{i}{2} \text{Tr}[Q(t, t) \gamma^q M_L], \quad (\text{A14})$$

leading to

$$I_L(t) = \frac{e}{2\hbar} \sum_k \sum_n \int \frac{d\omega}{2\pi} e^{in\Omega t} \text{Tr}[Q_{Lk,d}^K(n, \omega) M_L^{21} + Q_{d,Lk}^K(n, \omega) M_L^{12}], \quad (\text{A15})$$

where the trace over the lead-QD space has been performed, and the following identity was applied:

$$\text{Tr}[Q_\alpha \gamma^q] = Q_\alpha^K(t, t) = \sum_n \int \frac{d\omega}{2\pi} e^{in\Omega t} Q^K(n, \omega), \quad (\text{A16})$$

where Q^K is the Keldysh component of the Green's function. The above Green's functions (for the left lead) can be expressed as follows, in terms of the lead GF g_{Lk}^0 and dot GF Q_{dd} :

$$Q_{d,Lk} = M_T^{21} Q_{dd} \cdot g_{Lk}^0, \quad (\text{A17})$$

$$Q_{Lk,d} = M_T^{12} g_{Lk}^0 \cdot Q_{dd}. \quad (\text{A18})$$

Taking the Keldysh component of these products leads to

$$(Q_{d,Lk})^K = M_T^{21} [(Q_{dd})^R (g_{Lk}^0)^K + (Q_{dd})^K (g_{Lk}^0)^A], \quad (\text{A19})$$

and

$$(Q_{Lk,d})^K = M_T^{12} [(g_{Lk}^0)^R (Q_{dd})^K + (g_{Lk}^0)^K (Q_{dd})^A], \quad (\text{A20})$$

where $(Q, g^0)^{R/A}$ are the QD/lead Green's function retarded and advanced components. Upon substitution in Eq. A15, it leads to the following expression for the time-dependent current

$$I_L(t) = \frac{ie}{2\hbar} \sum_n e^{in\Omega t} \int \frac{d\omega}{2\pi} \Gamma_L \{ (1 - 2n_L(\omega)) \times [Q_{dd}^R(n, \omega) - Q_{dd}^A(n, \omega)] - Q_{dd}^K(n, \omega) \}, \quad (\text{A21})$$

where $n_L(\omega)$ is the Fermi-Dirac distribution of the L-lead. Note that, at this stage, the expression shows the exact current with its full time-dependence. The only assumption, as stated in the main text, is that the system is in a nonequilibrium steady-state, and thus the Green's function is periodic in time with the period τ of the drive. In addition, for the derivation of Eq. A21, the following are used:

- Identities for the lead GF, $(g_{Lk}^0(\omega))^K = -2\pi i \delta(\omega - \epsilon_k) [1 - 2n_L(\omega)]$ and $(g_{Lk}^0(\omega))^R - (g_{Lk}^0(\omega))^A = -2\pi i \delta(\omega - \epsilon_k)$.
- The summation over k is performed with the help of the δ -function, and we assume the wide-band limit for the leads, with a constant density of states $\rho(\omega) = \rho_{Fl}$.
- The line-width function is defined as $\Gamma_L = 2\pi \rho_{Fl} |\lambda_L|^2$.

The equivalent expression can also be derived for $I_R(t)$, defined as

$$I_R(t) = \frac{ie}{\hbar} \sum_{k\sigma} (\lambda_{Rk} l_{Rk\sigma}^\dagger d_\sigma - \lambda_{Rk\sigma}^* d_\sigma^\dagger l_{Rk\sigma}). \quad (\text{A22})$$

For a time-dependent system, $I_L(t) = -I_R(t)$ only holds for time averages, i.e. $\langle I_L(t) \rangle = -\langle I_R(t) \rangle$ [78].

Therefore, for the time-averaged current through the dot $\langle I \rangle = \langle (I_L - I_R)/2 \rangle$ the following simple expression for the current is valid:

$$\langle I \rangle = \frac{ie}{\hbar} \int \frac{d\omega}{2\pi} [n_F^L(\omega) - n_F^R(\omega)] \times \text{Tr} \left\{ \frac{\Gamma_L \Gamma_R}{\Gamma_L + \Gamma_R} [Q_{dd}^R(0, \omega) - Q_{dd}^A(0, \omega)] \right\}. \quad (\text{A23})$$

The above leads directly to the expression for the conductance of Eq. 9 in the main text.

-
- [1] N. Read and D. Green, *Phys. Rev. B* **61**, 10267 (2000).
 [2] A. Y. Kitaev, *Physics-Uspekhi* **44**, 131 (2001).
 [3] A. Y. Kitaev, *Annals of Physics* **303**, 2 (2003).
 [4] C. Nayak, S. H. Simon, A. Stern, M. Freedman, and S. Das Sarma, *Rev. Mod. Phys.* **80**, 1083 (2008).
 [5] J. M. Leinaas and J. Myrheim, *Il Nuovo Cimento B* (1971-1996) **37**, 1 (1977).
 [6] K. Fredenhagen, K.-H. Rehren, and B. Schroer, *Communications in Mathematical Physics* **125**, 201 (1989).
 [7] D. A. Ivanov, *Phys. Rev. Lett.* **86**, 268 (2001).
 [8] J. D. Sau, R. M. Lutchyn, S. Tewari, and S. Das Sarma, *Phys. Rev. Lett.* **104**, 040502 (2010).
 [9] R. M. Lutchyn, J. D. Sau, and S. Das Sarma, *Phys. Rev. Lett.* **105**, 077001 (2010).
 [10] Y. Oreg, G. Refael, and F. von Oppen, *Phys. Rev. Lett.* **105**, 177002 (2010).
 [11] J. Alicea, *Phys. Rev. B* **81**, 125318 (2010).
 [12] J. Alicea, *Reports on Progress in Physics* **75**, 076501 (2012).
 [13] V. Mourik, K. Zuo, S. M. Frolov, S. Plissard, E. P. Bakkers, and L. P. Kouwenhoven, *Science* **336**, 1003 (2012).
 [14] M. Deng, C. Yu, G. Huang, M. Larsson, P. Caroff, and H. Xu, *Nano letters* **12**, 6414 (2012).
 [15] A. Das, Y. Ronen, Y. Most, Y. Oreg, M. Heiblum, and H. Shtrikman, *Nature Physics* **8**, 887 (2012).
 [16] H. O. H. Churchill, V. Fatemi, K. Grove-Rasmussen, M. T. Deng, P. Caroff, H. Q. Xu, and C. M. Marcus, *Phys. Rev. B* **87**, 241401 (2013).
 [17] A. D. K. Finck, D. J. Van Harlingen, P. K. Mohseni, K. Jung, and X. Li, *Phys. Rev. Lett.* **110**, 126406 (2013).
 [18] S. M. Albrecht, A. P. Higginbotham, M. Madsen, F. Kuemmeth, T. S. Jespersen, J. Nygård, P. Krogstrup, and C. Marcus, *Nature* **531**, 206 (2016).
 [19] M. Deng, S. Vaitiekėnas, E. B. Hansen, J. Danon, M. Leijnse, K. Flensberg, J. Nygård, P. Krogstrup, and C. M. Marcus, *Science* **354**, 1557 (2016).
 [20] H. Zhang, Ö. Gül, S. Conesa-Boj, M. P. Nowak, M. Wimmer, K. Zuo, V. Mourik, F. K. De Vries, J. Van Veen, M. W. De Moor, *et al.*, *Nature communications* **8**, 1 (2017).
 [21] Ö. Gül, H. Zhang, J. D. Bommer, M. W. de Moor, D. Car, S. R. Plissard, E. P. Bakkers, A. Geresdi, K. Watanabe, T. Taniguchi, *et al.*, *Nature nanotechnology* **13**, 192 (2018).
 [22] H. Zhang, M. W. de Moor, J. D. Bommer, D. Xu, G. Wang, N. van Loo, C.-X. Liu, S. Gazibegovic, J. A. Logan, D. Car, *et al.*, *arXiv preprint arXiv:2101.11456* (2021).
 [23] Z. Wang, H. Song, D. Pan, Z. Zhang, W. Miao, R. Li, Z. Cao, G. Zhang, L. Liu, L. Wen, R. Zhuo, D. E. Liu, K. He, R. Shang, J. Zhao, and H. Zhang, *Phys. Rev. Lett.* **129**, 167702 (2022).
 [24] Z. Wang, S. Zhang, D. Pan, G. Zhang, Z. Xia, Z. Li, D. Liu, Z. Cao, L. Liu, L. Wen, D. Liao, R. Zhuo, Y. Li, D. E. Liu, R. Shang, J. Zhao, and H. Zhang, *Phys. Rev. B* **106**, 205421 (2022).
 [25] H. Song, Z. Zhang, D. Pan, D. Liu, Z. Wang, Z. Cao, L. Liu, L. Wen, D. Liao, R. Zhuo, D. E. Liu, R. Shang, J. Zhao, and H. Zhang, *Phys. Rev. Res.* **4**, 033235 (2022).
 [26] M. Aghaee *et al.*, (2022), 10.48550/ARXIV.2207.02472.
 [27] A. Eckardt, *Rev. Mod. Phys.* **89**, 011004 (2017).
 [28] T. Oka and S. Kitamura, *Annual Review of Condensed Matter Physics* **10**, 387 (2019), <https://doi.org/10.1146/annurev-conmatphys-031218-013423>.
 [29] M. S. Rudner and N. H. Lindner, *Nature reviews physics* **2**, 229 (2020).
 [30] A. Castro, U. De Giovannini, S. A. Sato, H. Hübener, and A. Rubio, *Phys. Rev. Research* **4**, 033213 (2022).
 [31] N. H. Lindner, G. Refael, and V. Galitski, *Nature Physics* **7**, 490 (2011).
 [32] T. Kitagawa, T. Oka, A. Brataas, L. Fu, and E. Demler, *Phys. Rev. B* **84**, 235108 (2011).
 [33] J. P. Dahlhaus, J. M. Edge, J. Tworzydło, and C. W. J. Beenakker, *Phys. Rev. B* **84**, 115133 (2011).
 [34] L. Jiang, T. Kitagawa, J. Alicea, A. R. Akhmerov, D. Pekker, G. Refael, J. I. Cirac, E. Demler, M. D. Lukin, and P. Zoller, *Phys. Rev. Lett.* **106**, 220402 (2011).
 [35] T. Kitagawa, M. A. Broome, A. Fedrizzi, M. S. Rudner, E. Berg, I. Kassal, A. Aspuru-Guzik, E. Demler, and A. G. White, *Nature communications* **3**, 1 (2012).
 [36] A. A. Reynoso and D. Frustaglia, *Phys. Rev. B* **87**, 115420 (2013).
 [37] D. E. Liu, A. Levchenko, and H. U. Baranger, *Phys. Rev. Lett.* **111**, 047002 (2013).
 [38] T. Iadecola, D. Campbell, C. Chamon, C.-Y. Hou, R. Jackiw, S.-Y. Pi, and S. V. Kusminskiy, *Phys. Rev. Lett.* **110**, 176603 (2013).
 [39] B. M. Fregoso, Y. H. Wang, N. Gedik, and V. Galitski, *Phys. Rev. B* **88**, 155129 (2013).
 [40] T. Iadecola, T. Neupert, and C. Chamon, *Phys. Rev. B* **89**, 115425 (2014).
 [41] L. E. F. Foa Torres, P. M. Perez-Piskunow, C. A. Balsero, and G. Usaj, *Phys. Rev. Lett.* **113**, 266801 (2014).
 [42] T. A. Sedrakyan, V. M. Galitski, and A. Kamenev, *Phys. Rev. Lett.* **115**, 195301 (2015).
 [43] M. C. Rechtsman, J. M. Zeuner, Y. Plotnik, Y. Lumer, D. Podolsky, F. Dreisow, S. Nolte, M. Segev, and A. Sza-

- meit, *Nature* **496**, 196 (2013).
- [44] A. C. Potter, T. Morimoto, and A. Vishwanath, *Phys. Rev. X* **6**, 041001 (2016).
- [45] R. Roy and F. Harper, *Phys. Rev. B* **96**, 155118 (2017).
- [46] R. W. Bomantara and J. Gong, *Phys. Rev. Lett.* **120**, 230405 (2018).
- [47] R. W. Bomantara and J. Gong, *Phys. Rev. B* **98**, 165421 (2018).
- [48] Y. Peng and G. Refael, *Phys. Rev. B* **98**, 220509 (2018).
- [49] Y. H. Wang, H. Steinberg, P. Jarillo-Herrero, and N. Gedik, *Science* **342**, 453 (2013), <https://www.science.org/doi/pdf/10.1126/science.1239834>.
- [50] F. Mahmood, C.-K. Chan, Z. Alpichshev, D. Gardner, Y. Lee, P. A. Lee, and N. Gedik, *Nature Physics* **12**, 306 (2016).
- [51] S. Aeschlimann, S. A. Sato, R. Krause, M. Chávez-Cervantes, U. De Giovannini, H. Hübener, S. Forti, C. Coletti, K. Hanff, K. Rossnagel, A. Rubio, and I. Gierz, *Nano Letters*, *Nano Letters* **21**, 5028 (2021).
- [52] T. Mori, T. Kuwahara, and K. Saito, *Phys. Rev. Lett.* **116**, 120401 (2016).
- [53] D. A. Abanin, W. De Roeck, W. W. Ho, and F. m. c. Huvneers, *Phys. Rev. B* **95**, 014112 (2017).
- [54] D. Abanin, W. De Roeck, W. W. Ho, and F. Huvneers, *Communications in Mathematical Physics* **354**, 809 (2017).
- [55] P. Ponte, A. Chandran, Z. Papić, and D. A. Abanin, *Annals of Physics* **353**, 196 (2015).
- [56] C. W. von Keyserlingk and S. L. Sondhi, *Phys. Rev. B* **93**, 245145 (2016).
- [57] J. Zhang, P. W. Hess, A. Kyprianidis, P. Becker, A. Lee, J. Smith, G. Pagano, I.-D. Potirniche, A. C. Potter, A. Vishwanath, et al., *Nature* **543**, 217 (2017).
- [58] S. Choi, J. Choi, R. Landig, G. Kucsko, H. Zhou, J. Isoya, F. Jelezko, S. Onoda, H. Sumiya, V. Khemani, et al., *Nature* **543**, 221 (2017).
- [59] B. Bauer, T. Pereg-Barnea, T. Karzig, M.-T. Rieder, G. Refael, E. Berg, and Y. Oreg, *Phys. Rev. B* **100**, 041102 (2019).
- [60] D. W. Hone, R. Ketzmerick, and W. Kohn, *Phys. Rev. E* **79**, 051129 (2009).
- [61] T. Iadecola, T. Neupert, and C. Chamon, *Phys. Rev. B* **91**, 235133 (2015).
- [62] D. E. Liu, *Phys. Rev. B* **91**, 144301 (2015).
- [63] K. I. Seetharam, C.-E. Bardyn, N. H. Lindner, M. S. Rudner, and G. Refael, *Phys. Rev. X* **5**, 041050 (2015).
- [64] Q. Yang, Z. Yang, and D. E. Liu, *Phys. Rev. B* **104**, 014512 (2021).
- [65] Z. Yang, Q. Yang, J. Hu, and D. E. Liu, *Phys. Rev. Lett.* **126**, 086801 (2021).
- [66] D. E. Liu, A. Levchenko, and R. M. Lutchyn, *Phys. Rev. B* **95**, 115303 (2017).
- [67] D. E. Liu and H. U. Baranger, *Phys. Rev. B* **84**, 201308 (2011).
- [68] G. Kells, D. Meidan, and P. W. Brouwer, *Phys. Rev. B* **86**, 100503 (2012).
- [69] C. Moore, T. D. Stanescu, and S. Tewari, *Phys. Rev. B* **97**, 165302 (2018).
- [70] C. Moore, C. Zeng, T. D. Stanescu, and S. Tewari, *Phys. Rev. B* **98**, 155314 (2018).
- [71] A. Vuik, B. Nijholt, A. R. Akhmerov, and M. Wimmer, *SciPost Phys.* **7**, 061 (2019).
- [72] D. Liu, Z. Cao, X. Liu, H. Zhang, and D. E. Liu, *Phys. Rev. B* **104**, 205125 (2021).
- [73] H. Pan and S. Das Sarma, *Phys. Rev. Research* **2**, 013377 (2020).
- [74] O. Shtanko and R. Movassagh, *Phys. Rev. Lett.* **125**, 086804 (2020).
- [75] D. E. Liu, M. Cheng, and R. M. Lutchyn, *Phys. Rev. B* **91**, 081405 (2015).
- [76] A. Kamenev, *Field Theory of Non-Equilibrium Systems* (Cambridge University Press, 2011).
- [77] A. Altland and B. D. Simons, *Condensed Matter Field Theory*, 2nd ed. (Cambridge University Press, 2010).
- [78] H. Haug, A.-P. Jauho, et al., *Quantum kinetics in transport and optics of semiconductors*, Vol. 2 (Springer, 2008).